Journal of Physiology (1991), **437**, *pp.* 655–672
With 6 figures
Printed in Great Britain

FORCE–VELOCITY RELATIONS AND MYOSIN HEAVY CHAIN ISOFORM COMPOSITIONS OF SKINNED FIBRES FROM RAT SKELETAL MUSCLE

BY R. BOTTINELLI, S. SCHIAFFINO* AND C. REGGIANI

*From the Institute of Human Physiology, via Forlanini 6, I-27100 Pavia, Italy and *CNR Unit for Muscle Biology and Physiopathology, Institute of General Pathology, University of Padova, Italy*

(*Received 10 April 1990*)

SUMMARY

1. This study was performed to assess whether muscle contractile properties are related to the presence of specific myosin heavy chain (MHC) isoforms.

2. Force–velocity relations and MHC isoform composition were determined in seventy-four single skinned muscle fibres from rat soleus, extensor digitorum longus and plantaris muscles.

3. Four groups of fibres were identified according to their MHC isoform composition determined by monoclonal antibodies: type 1 (slow), and types 2A, 2B and 2X (fast).

4. With respect to maximum velocity of shortening (V_0), the fibres formed a continuum between 0·35 and 2·84 L/s (muscle lengths per second) at 12 °C. V_0 in type 1 fibres (slow fibres) was between 0·35 and 0·95 L/s (0·639 ± 0·038 L/s; mean ± S.E. of mean). V_0 in type 2 fibres (fast fibres) was consistently higher than 0·91 L/s. Ranges of V_0 in the three fast fibre types mostly overlapped. Type 2A and 2X fibres had similar mean V_0 values (1·396 ± 0·084 and 1·451 ± 0·066 L/s respectively); type 2B fibres showed a higher mean V_0 value (1·800 ± 0·109 L/s) than type 2A and 2X fibres.

5. Mean values of a/P_0^*, an index of the curvature of force–velocity relations, allowed us to identify two groups of fibres: a high curvature group comprised of type 1 (mean a/P_0^*, 0·066 ± 0·007) and 2A (0·066 ± 0·024) fibres and a low curvature group comprised of type 2B (0·113 ± 0·013) and 2X (0·132 ± 0·008) fibres.

6. Maximal power output was lower in slow fibres than in fast fibres, and among fast fibres it was lower in type 2A fibres than in type 2X and 2B.

7. Force per unit cross-sectional area was less in slow fibres than in fast fibres. There was no relation between fibre type and cross-sectional area.

8. The results suggest that MHC composition is just one of the determinants of shortening velocity and of other muscle contractile properties.

INTRODUCTION

Myosin has been the most extensively studied among the contractile proteins in relation to the heterogeneity in shortening velocity and ATPase activity among mammalian skeletal muscle fibres. Myosin consists of six subunits – two heavy

chains and two pairs of light chains – and can exist in multiple isoforms due to variations in both its heavy (MHC) and light chain (MLC) subunits.

Three muscle fibre types (1, 2A and 2B) can be histochemically identified in mammalian skeletal muscles using assays for myosin ATPase activity (Brooke & Kaiser, 1970). This characterization has been shown to be related to MHC composition (Staron & Pette, 1986). Recently three MHC isoforms have been separated using improved electrophoretic techniques (Danieli-Betto, Zerbato & Betto, 1986), and it has been demonstrated that they are coded for by three different genes (Izumo, Nadal Ginard & Mahdavi, 1986). Evidence for a fourth MHC isoform called type 2X (Schiaffino, Saggin, Viel, Ausoni, Sartore & Gorza, 1986; Schiaffino, Gorza, Sartore, Saggin, Ausoni, Vianello, Gundersen & Lømo, 1989) or 2D (Bar & Pette, 1988) has been presented.

Six MLC isoforms are expressed in skeletal muscle: MLC1f, MLC3f (or alkali MLCs) and MLC2f (or DTNB MLC) in fast muscle, and MLC1sa, MLC1sb (homologous to the alkali MLCs) and MLC2s (homologous to the DTNB MLC) in slow muscle.

Two MHCs associate with two alkali light chains in various proportions (i.e. in fast muscle: LC1f:LC3f; LC1f:LC1f; LC3f:LC3f) and with two MLC2s. Different MHCs can co-exist in the same fibre (Danieli-Betto *et al.* 1986; Staron & Pette, 1987*a*, *b*; Termin, Staron & Pette, 1989). Fast MLCs can occasionally co-exist with slow MHCs (Staron & Pette, 1987*a*). In conclusion, when analysed according to myosin isoforms, muscle fibres appear as a continuum, rather than the three or four discrete types that might be inferred from histochemical analysis of ATPase activity.

Many studies have tried to correlate contractile performance with MHC and MLC composition. A relation between shortening velocity and ATPase activity and MHC isoform composition has been found in studies performed on rat ventricular myocardium (Mercandier, Lompre, Wisnewsky, Samuel, Bercovici, Swinghedauw & Schwartz, 1981), rabbit single skinned muscle fibres (Reiser, Moss, Giulian & Greaser, 1985), avian single skinned fibres (Reiser, Greaser & Moss, 1988) and frog muscle fibres (Edman, Reggiani, Schiaffino & te Kronnie, 1988). Recent studies, however, have shown a large variability in shortening velocity among mammalian fibres containing fast MHC (Greaser, Moss & Reiser, 1988). Variation in the relative content of the MLC isoforms can at least partially explain such a variability (Greaser *et al.* 1988; Sweeney, Kushmerick, Mabuchi, Sréter & Gergely, 1988). An alternative or complementary explanation might be represented by the presence of undetected MHC isoforms. The fast isoforms of MHCs are difficult to distinguish and the presence of one or even more of them can be overlooked.

This work aimed to study in greater detail the role of MHCs in determining the contractile properties of mammalian skeletal muscle fibres. To this end, force–velocity relations were determined in single skinned muscle fibres from rat soleus, extensor digitorum longus (EDL) and plantaris muscles. MHC isoforms in the same fibres were thereafter identified using six monoclonal antibodies directed against MHC isoforms. This immunohistochemical method very precisely identifies the predominant MHC isoform. Beside the slow MHC, three fast MHC isoforms (type 2A, 2B and the still poorly defined 2X) were recognized and related to the force–velocity properties of single fibres.

METHODS

Fibre dissection

Experiments were performed on single fibres from EDL, soleus and plantaris muscles of 3-month-old male Wistar rats. After the animal had been killed, the muscles were dissected free and immersed in skinning solution at 12–15 °C for 2–4 h. During this time segments of single fibres were isolated using a stereomicroscope (Wild 10–40 ×), and care was taken to avoid undue stretching. At the end of this period the solution was replaced with a fresh skinning solution containing Triton X-100. Aluminium foil clips were attached to both ends of the fibre segment which was then transferred to the experimental set-up. Fibres were always used on the day of dissection.

Solutions

Skinning, relaxing, pre-activating and activating solutions were prepared according to Brenner (1983) with some modifications (see Table 1). Two skinning solutions were employed: the first had the composition reported in Table 1 and the second also contained Triton X-100 (BDH chemicals Poole, UK) (0·5 μl/ml) to ensure complete skinning. The pCa of the activating solution was estimated to be 4·45 on the basis of a computer program designed by Fabiato (Fabiato, 1988); pMg and pMgATP in the activating solution were calculated in the same way. Both activating and pre-activating solutions contained caffeine (10 mM) and a rephosphorylating system based on creatine phosphokinase (Boehringer Mannheim, Germany) (300 U/ml) and creatine phosphate (Boehringer Mannheim, Germany) (25 mM). Caffeine was used to inhibit Ca^{2+} uptake by the sarcoplasmic reticulum and thus to prevent tension oscillations during activation should the Triton X-100 concentration be insufficient to completely disrupt the sarcoplasmic reticulum. The high concentration of creatine phosphokinase and creatine phosphate ensured optimal energy supply to the fibres even during prolonged maximal activation. Lower concentrations of creatine phosphokinase and creatine phosphate resulted in a decrease in shortening velocity, as observed in pilot experiments.

Experimental set-up

The experimental set-up was composed of three chambers milled into a Perspex plate, which could be lowered and translated to quickly immerse the fibre in any of the three chambers. The first chamber (volume 3 ml) contained relaxing solution and was used for fibre mounting. The second and third chambers contained 1 ml of pre-activating and activating solutions respectively. The walls of the chambers were surrounded by channels for circulation of the water–glycol solution used for temperature control. In all experiments, the temperature in the experimental chamber was kept at 12 °C using an Endocal Neslab thermostat. The fibre segments were mounted horizontally between an electromagnetic puller (Ling 101 vibrator) and a force transducer (AE 801 Aksjeselskapet Mikroelektronikk, Horten, Norway, resonance frequency in water 2 kHz). During the mounting procedure fibres were viewed through a stereomicroscope (Wild 10–40 ×) fitted over the apparatus. The segment was positioned to prevent sideways movements or torsion during activation and experimental manoeuvres. The electromagnetic puller, which was provided with an inductance position transducer, was driven by a feedback circuit whose input was either the output of the position transducer (length control mode) or the output of the force transducer (load-control mode). In the former, the length of the segment was kept constant to obtain isometric contractions. In the latter, load was controlled so that records of isotonic shortening against different loads could be obtained.

Experimental procedure

At the beginning of the experiment, the fibre segment was mounted in the chamber containing relaxing solution. Segment length was measured at 40 × magnification through the stereomicroscope and was always set at 1·1 times slack length. In fifteen experiments the experimental set-up was placed on the stage of an inverted microscope and sarcomere length was measured before activation at 320 × magnification. The length at which the segment was set (1·1 times slack length) was found to correspond to a sarcomere length of $2{\cdot}50 \pm 0{\cdot}048$ μm (mean ± S.E. of mean). Maximal activation was induced by transferring the fibre segment from the chamber containing pre-activating (Ca^{2+}-free) solution to the chamber containing activating solution. Tension rose to a steady value that was generally maintained throughout activation, which usually lasted 3–5 min.

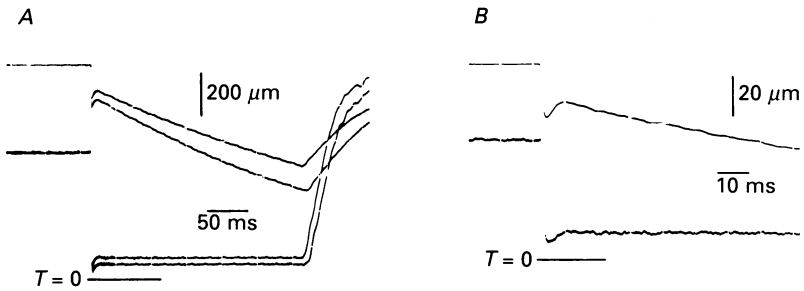

Fig. 1. Examples of load-clamp recordings during continuous maximal activation of segments of single skinned muscle fibres. Upper traces, segment length; lower traces, force; $T = 0$ marks zero force. Temperature, 12 °C. *A*, two load clamps at two different force levels. Segment of plantaris fibre; segment length = 1·619 mm. *B*, a load clamp of a segment of plantaris fibre; segment length = 1·281 mm. Note the different time base: the calibration bar corresponds to 50 ms in *A*, and to 10 ms in *B*.

TABLE 1. Composition of solutions (in mM)

Solution	KCl	Imidazole	$MgCl_2$	NaATP	EGTA	$CaCl_2$	DTT	CrP	CPK*	Caffeine
Relaxing solution	100	20	5	5	5	—	1	—	—	—
Pre-activating solution	100	20	5	5	5	—	1	25	300	10
Activating solution	100	20	5	5	5	5	1	25	300	10
	K Prop	KH_2PO_4	MgAc							
Skinning solution	150	5	5	3	5	1	1	—	—	—

In the activating solution: pCa = 4·45, pMgATP = 2·40, pMg = 3·14.

* In U/ml, where one unit transfers 1·0 μmol of phosphate from CrP to ADP per minute at pH 7·4 and 30 °C. Abbreviations: DTT, dithiothreitol; CrP, creatine phosphate; CPK, creatine phosphokinase; K Prop, potassium propionate; MgAc, magnesium acetate.

During activation tension did not decrease by more than 10% of the initial value. Once activated the specimen was subjected to a series (fifteen to twenty-five) of load clamps at 5 s intervals to obtain the force–velocity relation. The same load clamps (i.e. isotonic shortening against the same load) were repeated at the beginning and at the end of the experiment (see below). Relaxation was obtained by returning the fibre segment to the chamber containing pre-activating (Ca^{2+}-free) solution, and finally to the chamber containing relaxing solution. At the end of the experiment the fibre segment was removed from the apparatus and put in a small Petri dish filled with relaxing solution containing gelatine (15%) at 37 °C. After allowing the gelatine to set for 30 min at 4 °C, the block of gelatine containing the piece of fibre was cut out and frozen in liquid nitrogen for subsequent immunocytochemical analysis.

Data recording and analysis

The outputs of the force transducer and of the position transducer were displayed on a storage oscilloscope (model 5113, Tektronix, Beaverton, Oregon, USA) and on a chart recorder (Graphtec WR3701, Japan). Analyses were carried out mostly on the chart recorder outputs; however, photographs of the oscilloscope screen were often taken and utilized for measurements. Examples of representative experimental records are shown in Fig. 1.

Shortening velocity was measured by linear interpolation in the interval between 30 and 40 ms after the beginning of the load clamp and was expressed in segment lengths per second (L/s). Force was expressed as P/P_0, where P is the force during the load clamp and P_0 is the isometric tension generated by the fibre just prior to load clamping. Hill's hyperbolic equation was fitted to all experimental data points according to a minimization procedure derived from that described by Edman, Mulieri & Scubon-Mulieri (1976). The numerical values of maximum shortening velocity (V_0), a/P_0 and P_0^* (i.e. the intercept of the computed force–velocity curve with the force axis), were

calculated. The value of a/P_0^* was used to quantify the curvature of the force–velocity relation. Using P_0^*, V_0 and a/P_0^*, maximum power output was computed for each fibre. Two different values were calculated (Woledge, Curtin & Homsher, 1985): P_{max}^{**}, maximal power output expressed relative to both P_0 and V_0 (units, P_0V_0), and P_{max}^*, maximal power output expressed relative to P_0

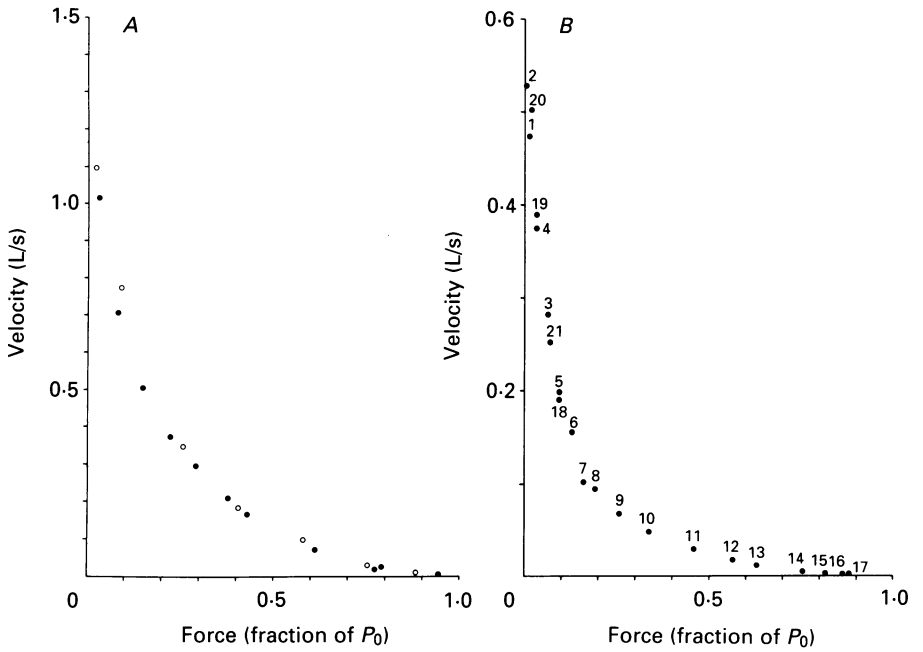

Fig. 2. Force–velocity relations from load-clamp recordings of two segments of single skinned muscle fibres showing two of the quality control procedures used. Segment length was set at 1·1 times slack length. Velocity is expressed in L/s and force in fraction of P_0. Temperature, 12 °C. *A*, force–velocity points obtained during two subsequent maximal activations in the same fibre segment. Filled circles (first activation) and open circles (second activation) are almost superimposed. Type 2B fibre: $V_0 = 1{\cdot}290$ L/s; $a/P_0^* = 0{\cdot}161$. *B*, force–velocity points obtained in the order indicated by the numbers (1–21) during the same maximal activation. Force–velocity points obtained at the end of the activation (18–21) are similar to those obtained at the beginning of the activation (1–6). Type 1 fibre: $V_0 = 0{\cdot}628$ L/s; $a/P_0^* = 0{\cdot}066$.

(units, P_0 L/s). The former depends only on the curvature of the force–velocity relation, while the latter depends also on maximum shortening velocity. Maximum shortening velocity was also evaluated by linear extrapolation of data points below 0·1 P_0 (V_0(lin)).

Quality controls

Disorder of the contractile material can easily develop during prolonged and maximal activation of skinned muscle fibres. This might affect shortening velocity and make our data less reliable. The quick and uniform activation was designed to avoid gross non-uniformities in the behaviour of different areas of our specimens.

Additional measures were taken to ensure that our specimens did not undergo massive sarcomere disorganization:

(1) Several fibres were subjected to two maximal and prolonged activations lasting about 3 min at intervals of several minutes, and force–velocity curves were obtained during both activations and thereafter compared (Fig. 2*A*). The force–velocity curves obtained during the two activations were superimposable. This result ensured that following the first activation the capacity of the fibre to shorten was not impaired.

(2) Our experimental procedure (see above) was such that the fibre was subjected to the same load clamps at the beginning and at the end of activation. Data points obtained at the beginning and at the end of activation were superimposable (Fig. 2*B*).

(3) Direct observation of the fibre through a stereomicroscope showed that no gross inhomogeneities in fibre diameter developed during activation.

TABLE 2. Pattern of reactivity of the six monoclonal antibodies with different isoforms of myosin heavy chains

MHC isoform	BF-G6	BF-35	BA-F8	SC-71	BF-49	BF-13
1 or slow	−	+	+	−	+	−
2A	−	+	−	+	+	+
2B	+	+	−	−	+	+
2X	−	−	−	−	+	+

(4) A number of experiments were carried out with the experimental set-up placed on the stage of an inverted microscope. Striation pattern was checked before and after each activation at 320 × magnification. The experimental set-up did not allow us to check the striation pattern during activation as the laser beam could not be projected through the chamber containing activating solution. A few fibres displayed disordered striation patterns after activation and were discarded.

(5) Fibres in which force during activation decreased by more than 10% of initial force were discarded, as well as fibres that did not relax completely at the end of activation. This latter event took place very rarely, whereas the former occurred somewhat more often.

Statistical analysis

Data were expressed as means and standard errors of means (S.E.M.). Statistical significance of the differences between means was determined by Student–Newman–Keuls' test after an analysis of variance. A probability of less than 5% was considered to be statistically significant. The statistical package 'Primer in Biostatistics' (by S. A. Glantz, released by McGraw-Hill INC 1989) was used.

Immunocytochemistry

Monoclonal antibodies against myosin heavy chains were obtained as described by Schiaffino *et al.* (1989). Six different antibodies were used to identify four different MHC isoforms; the specific activities of the six antibodies are reported in Table 2, and shown in Fig. 3. Bound antibodies were revealed by immunoperoxidase staining.

Antibody reactivity was assessed on thin (10 μm) cross-cryosections of individual fibre segments. On each slide cross-cryosections of whole muscles (soleus, EDL, plantaris) from the same animal were incubated together with single-fibre sections. This was done to ensure that the staining procedure worked satisfactorily. Fiber diameter and cross-sectional area were determined on antibody-reacted cross-sections using a computerized image analyser (IBAS, Kontron Byldanalyse, Munich, Germany).

Monoclonal antibodies identified one slow and three fast MHC isoforms (Table 2). This represents an improvement compared to previous studies in which shortening velocity was related to MHC composition; no more than two isoforms were electrophoretically identified by Reiser *et al.* (1985), Sweeney *et al.* (1988) and Greaser *et al.* (1988). A limitation of the immunohistochemical method is its inability to precisely resolve MHC co-existence. Different MHC isoforms can co-exist in the same fibre (Danieli-Betto *et al.* 1986; Staron & Pette, 1987*a*, *b*). In normal adult rat muscles type 2A MHC can co-exist with type 1 and 2X MHC, and type 2X MHC can co-exist with type 2B MHC (Termin *et al.* 1989). In chronically stimulated fast rat muscles all MHCs can co-exist with one another (Termin *et al.* 1989). Monoclonal antibodies cannot detect the co-existence of type 2A with 2X or of type 2X with 2B MHC, as none of the antibodies specifically stains type 2X MHC. Identification of type 2X MHC is obtained by negative staining with the other antibodies used. Monoclonal antibodies should uncover the co-existence of type 2A with 2B or with type 1 MHC. Fibres containing type 2A and 2B or type 2A and 1 MHC should react with more than one specific

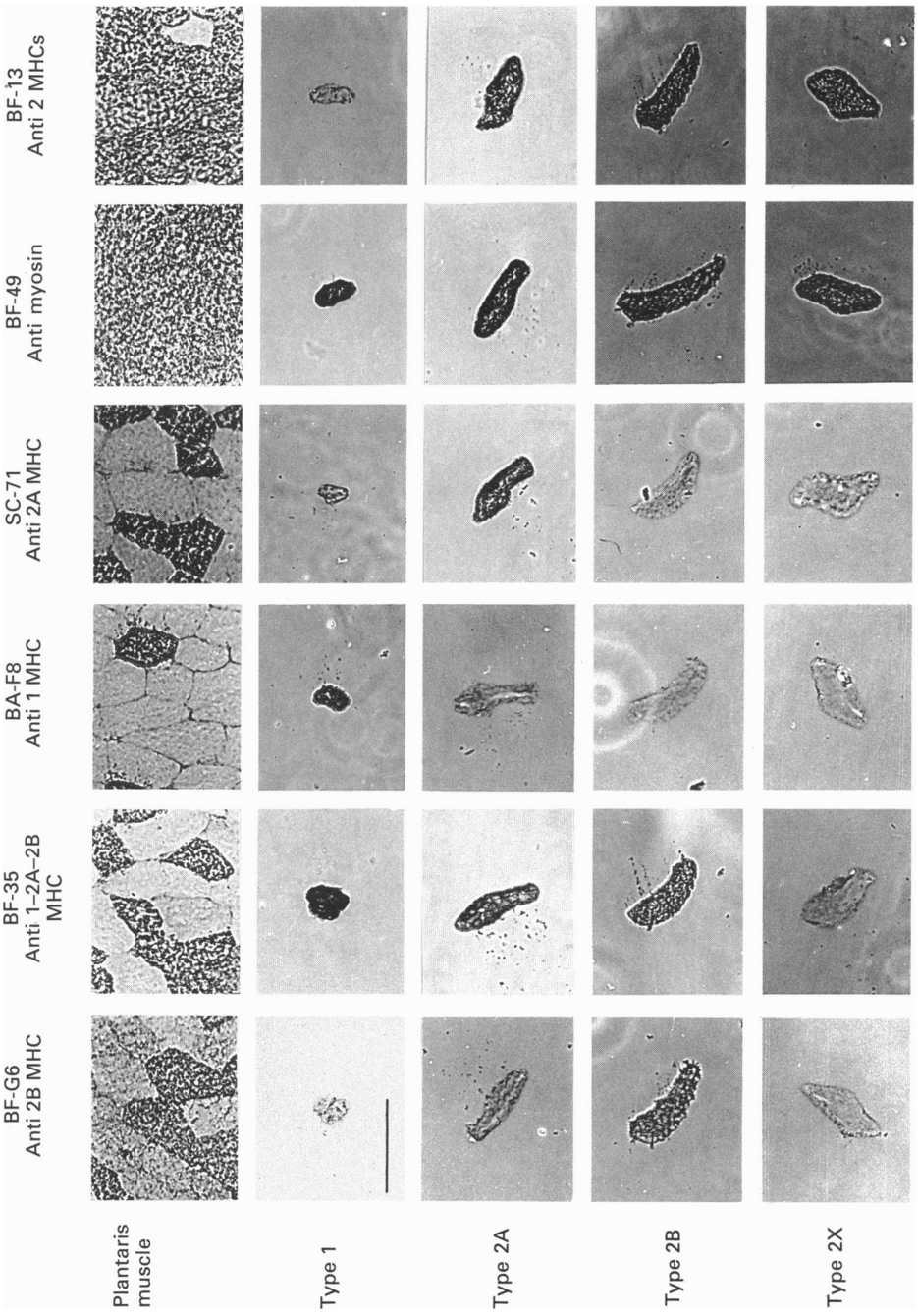

Fig. 3. Immunoperoxidase staining of cross-cryosections of one representative fibre per type and of a small area of a whole plantaris muscle. Phase-contrast microscope was used. The calibration bar in the first picture from the left of the type 1 fibre corresponds to 100 μm. For the antibody reactivity see Table 2. Due to the automatic exposure of the camera the intensity of staining of the cryosections of the single fibres is not readily comparable with that of the cryosections of the whole muscle.

antibody. The resolution of the antibody technique in detecting small amounts of a MHC isoform co-existing with a predominant MHC isoform is, however, difficult to assess.

RESULTS

Immunocytochemical fibre typing

Four fibre types were identified according to their MHC isoform composition: type 1 (slow, see below), and types 2A, 2B and 2X (fast, see below). As can be seen easily (Table 2; Fig. 3) all fibre types stained with BF-49 and all type 2 fibres stained with BF-13; each fibre type was specifically stained by one antibody except type 2X. Type 2X fibres were identified by their staining with BF-49 and BF-13 and not with the other antibodies.

Monoclonal antibodies do not detect the co-existence of type 2X with 2A or 2B MHC (see Methods). Fibres identified as type 2A or 2B might contain various amounts of type 2X MHC. On the other hand, the antibody staining should uncover the co-existence of type 2A with type 1 MHC or 2B MHC (see Methods). All type 1 fibres contained only type 1 MHC. No fibres with a mixture of type 2A and 2B MHC were found. Type 2X fibres should contain only type 2X MHC as they were identified by lack of staining with the specific antibodies used against type 1, 2A and 2B MHCs. As stated in Methods, the resolution of the antibody technique is difficult to assess. It might be that small amounts of a MHC isoform co-existing with a predominant one were overlooked.

Table 3 presents maximum shortening velocity (V_0), a/P_0^*, maximum power outputs (P^*_{max} and P^{**}_{max}), cross-sectional area (CSA) and isometric force (P_0) values for the four fibre types.

Cross-sectional area and force

Cross-sectional area was measured from the antibody-stained cryosections of fibre segments that had been mechanically characterized. Measurements were not corrected for possible swelling during skinning (Godt & Maughan, 1977) or shrinkage during gelatine embedding. Cross-sectional area values were only used for comparison. No significant differences were found among the different fibre types.

Force developed per unit of cross-sectional area (P_0) was significantly less in type 1 than in type 2X and 2B fibres. Type 2A and 2B fibres showed intermediate values between type 1 and 2X fibres. However, no significant difference was found among fast fibres.

Force–velocity relation

Curvature of force–velocity relation

Figure 4 shows force–velocity relations from single representative fibres of each immunohistochemical type. It can be seen that the curvature of the force–velocity relationship varied in different fibre types being more pronounced for type 1 (Fig. 4*A*) and 2A (Fig. 4*B*) than for type 2B (Fig. 4*C*) and 2X (Fig. 4*D*). The curvature of the force–velocity relation was quantified for each fibre by the parameter a/P_0^* of Hill's hyperbolic equation (Table 3). Type 2B fibres displayed the widest range of a/P_0^* values (0·034–0·264). Types 2A (0·029–0·120) and 1 (0·015–0·123) had a/P_0^* ranges which overlapped the lower part of the range for type 2B fibres. Type 2X fibres had higher a/P_0^* values (0·067–0·197). Two different groups of fibres were separated on

TABLE 3. Size and contractile parameters of the fibre population examined in this study. The fibres are classified according to MHC isoform composition

MHC isoform	CSA (μm^2)	Isometric force (kN/m^2)	V_0 (L/s)	a/P_0^*	P^*_{max} (P_0 L/s)	P^{**}_{max} (P_0 V_0)	n
1	1668·25 ± 134·21	211·44 ± 24·00	0·639 ± 0·038 (0·35–0·95)	0·066 ± 0·007 (0·015–0·123)	0·029 ± 0·002	0·037 ± 0·003	19
2A	1284·37 ± 247·82	303·50 ± 65·71	1·396 ± 0·084 (1·10–1·67)	0·066 ± 0·024 (0·029–0·102)	0·063 ± 0·007	0·042 ± 0·004	8
2X	1691·38 ± 566·56	439·01 ± 31·63	1·451 ± 0·066 (0·91–1·94)	0·132 ± 0·008 (0·067 ± 0·197)	0·093 ± 0·005	0·059 ± 0·002	19
2B	1844·22 ± 216·95	337·74 ± 35·78	1·800 ± 0·109 (0·93–2·84)	0·113 ± 0·013 (0·034 ± 0·264)	0·093 ± 0·005	0·051 ± 0·003	28
1 *vs.* 2A	n.s.	n.s.	s	n.s.	s	n.s.	
1 *vs.* 2X	n.s.	s	s	s	s	s	
1 *vs.* 2B	n.s.	s	s	s	s	s	
2A *vs.* 2X	n.s.	n.s.	n.s.	s	s	n.s.	
2A *vs.* 2B	n.s.	n.s.	s	s	s	n.s.	
2X *vs.* 2B	n.s.	n.s.	s	n.s.	n.s.	n.s.	

All values are given as means and standard errors. Ranges are reported for V_0 and a/P_0^* in parentheses. Statistical significance of the differences was determined by variance analysis followed by Student–Newman–Keuls' test. Abbreviations: CSA, cross-sectional area; V_0, maximum shortening velocity; P^*_{max}, maximum power output expressed relative to P_0 (isometric tension); P^{**}_{max}, maximum power output expressed relative to P_0 and V_0; n, number of fibres; s, statistically significant; n.s., non-significant.

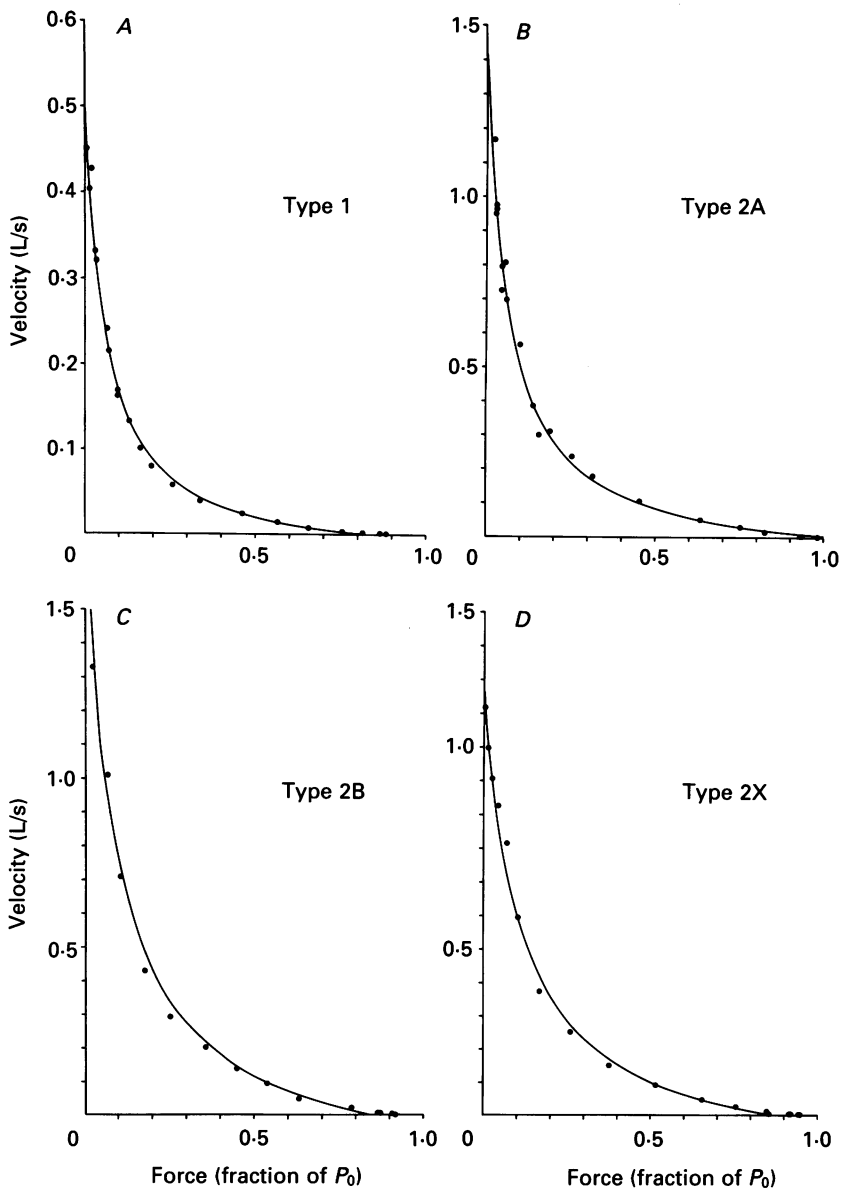

Fig. 4. Examples of force–velocity relations from load-clamp recordings from segments of skinned fibres representative of each of the immunocytochemical types. Hill's characteristic equation was used to obtain the fitted hyperbolae and the values of V_0, P_0^* and a/P_0. Velocity is expressed in L/s, force in fraction of P_0. Temperature, 12 °C. *A*, type 1 fibre, $V_0 = 0{\cdot}535$ L/s, $a/P_0^* = 0{\cdot}066$, $P_0^*/P_0 = 0{\cdot}829$. *B*, type 2A fibre, $V_0 = 1{\cdot}449$ L/s, $a/P_0^* = 0{\cdot}053$, $P_0^*/P_0 = 1{\cdot}134$. *C*, type 2B fibre, $V_0 = 1{\cdot}769$ L/s, $a/P_0^* = 0{\cdot}110$, $P_0^*/P_0 = 0{\cdot}861$. *D*, type 2X fibre, $V_0 = 1{\cdot}258$ L/s, $a/P_0^* = 0{\cdot}129$, $P_0^*/P_0 = 0{\cdot}887$. As indicated by the a/P_0^* values, curvature of the force–velocity relation was higher for type 1 and 2A fibres than for type 2B and 2X fibres.

the basis of mean a/P_0^* values. Types 1 and 2A displayed significantly lower mean values (0·066 for both types) and therefore more pronounced curvature of the force–velocity relation than types 2B and 2X (0·113 and 0·132 respectively). It is interesting to note that types 2A and 2X had very similar shortening velocities, but

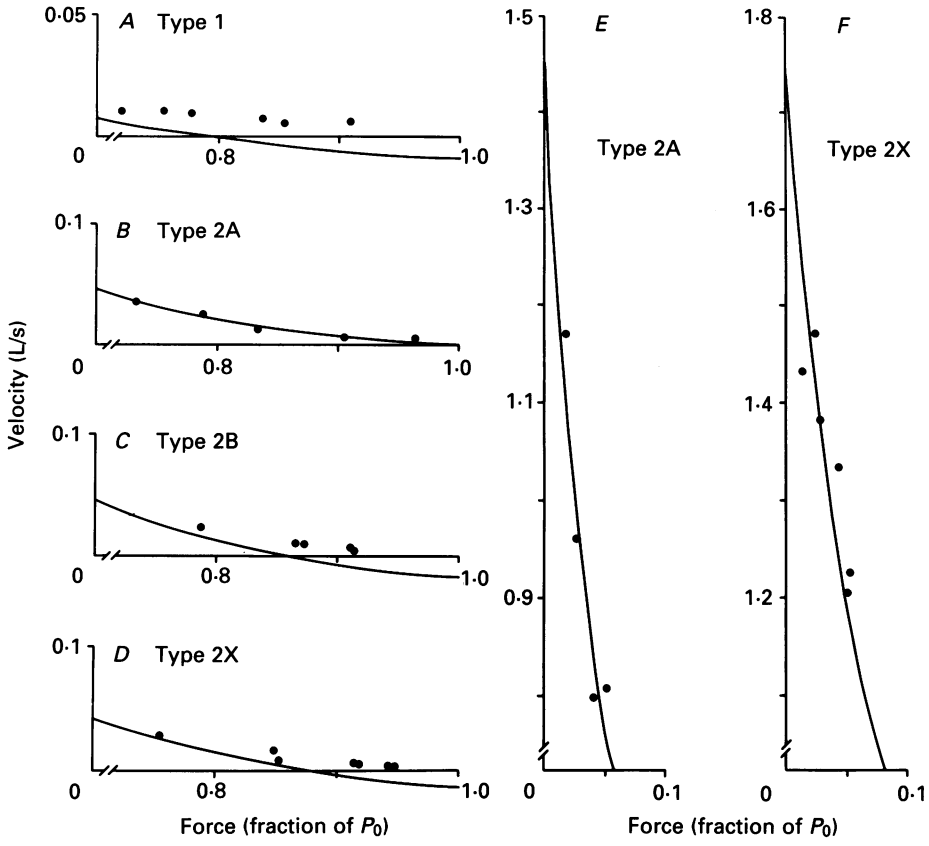

Fig. 5. Expanded views of force–velocity relations at high loads (above 0·7 P_0) (*A*, *B*, *C* and *D*) and at low loads (below 0·1 P_0) (*E* and *F*). Hyperbolic curves, P_0^* and V_0 values were obtained by fitting Hill's characteristic equation; V_0(lin) values were obtained by linear extrapolation of data points below 0·1 P_0. *A*, type 1 fibres, $P_0^* = 0{\cdot}789$. *B*, type 2A fibre, $P_0^* = 0{\cdot}989$. *C*, type 2B fibre, $P_0^* = 0{\cdot}861$. *D*, type 2X fibre, $P_0^* = 0{\cdot}887$. *E*, type 2A fibre, $V_0 = 1{\cdot}449$ L/s, V_0(lin) = 1·303 L/s. *F*, type 2X fibre, $V_0 = 1{\cdot}739$ L/s, V_0(lin) = 1·599 L/s.

were significantly different on the basis of the curvature of the force–velocity relation.

Shape of the force–velocity relation

Figure 5*A–D* presents the high-load portion of the force–velocity curve; it can be seen that for type 1, 2B and 2X fibres at high loads (above 0·8 P/P_0) force–velocity points departed from the hyperbolic curve fitted to all data using Hill's equation. Data points at high loads consistently fell above the fitted hyperbolae for type 1, 2B and 2X fibres and mean P_0^* values were significantly lower ($P_0^*/P_0 = 0{\cdot}879 \pm 0{\cdot}012$, mean ± S.E.M., $n = 63$) than actual isometric force (P_0). On the other hand, mean P_0^*

values computed for type 2A fibres were very close to the isometric force (P_0^*/P_0 = 1·027 ± 0·054, mean ± S.E.M., $n = 8$), and data points at high loads did not depart from the hyperbola (see Fig. 5*B*).

Figure 5*E* and *F* shows the low-load portion of the force–velocity curves from two representative fibres. In these two fibres, as in all fibres studied, data points at low

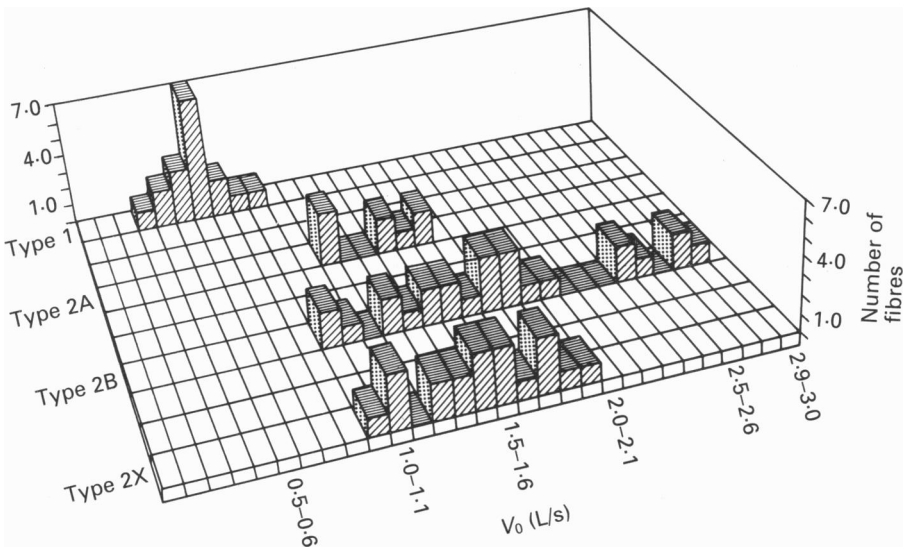

Fig. 6. Distribution of maximum shortening velocities in the four types of single skinned muscle fibres identified by monoclonal antibodies. The height of each vertical bar represents the number of fibres of each type for which V_0 was found to occur in each 0·1 L/s increment. *X*-axis, V_0 L/s; *Y*-axis, number of fibres; *Z*-axis, fibre type.

loads did not significantly depart from the hyperbola. Linear extrapolation of data points below 0·1 P/P_0 gave V_0 values consistently lower than those obtained by Hill's equation, by an average (± S.E.M.) of 13·13 ± 1·55 % V_0 ($n = 63$).

Maximum shortening velocity

Table 3 presents means and ranges of maximum shortening velocity of the four fibre types. There was a clear difference between slow (type 1) and fast (type 2) fibres: V_0 for type 1 fibres was between 0·35 and 0·95 L/s and V_0 for type 2 (A, B, X) fibres was between 0·91 and 2·84 L/s.

Type 2 fibres had overlapping ranges of V_0. Type 2B fibres encompassed the entire range of velocities (0·93–2·84 L/s), whereas types 2A and 2X had almost identical velocity ranges (1·10–1·67 and 0·91–1·94 L/s respectively). Thus only type 2B fibres had V_0 values higher than 1·94 L/s, while all three fast fibre types had V_0 values in the range 0·91–1·94 L/s.

Mean values of maximum shortening velocities showed that type 1 fibres were the slowest (0·64 L/s); type 2B (1·80 L/s) were faster than the other fast fibres, whereas type 2A (1·40 L/s) and 2X (1·45 L/s) had almost the same mean V_0.

Figure 6 shows the distribution of V_0 in the four fibre types. The height of each vertical bar represents the number of fibres for which V_0 was a particular value. The

histogram provides further insight into the distribution of maximum shortening velocities. Two points deserve comment. First, there is large variability in V_0 not only among fibres on the whole, but also within each fibre type. Second, the V_0 distribution of type 2B fibres seem to be bimodal (nineteen fibres in the range 0·90–2·10 L/s, and six fibres in the range 2·4–2·9 L/s).

Maximum power output

Two different values of maximum power output were calculated (Table 3): P^{**}_{max} expressed relative to P_0 and V_0, and P^{*}_{max} expressed relative only to P_0. The value of P^{*}_{max} was significantly lower in slow fibres (0·029 P_0 L/s) than in fast fibres. Among fast fibres type 2B and 2X fibres had values (0·093 P_0 L/s for both types) that were higher than type 2A fibres (0·063 P_0 L/s). The same was true with P^{**}_{max} values even though the differences were somewhat less pronounced. Thus while type 2A and 2X fibres displayed almost identical mean shortening velocities, they were different in mean maximal power output and in mean a/P^{*}_{0} (see above).

DISCUSSION

Cross-sectional area and isometric force development

A wide population of muscle fibres belonging to EDL, soleus and plantaris muscles was examined in this study. Force–velocity relations and MHC isoforms were determined for each fibre.

Cross-sectional area was not found to be significantly different for different fibre types. This was in contrast with previous studies on rat diaphragm (Eddinger & Moss, 1987) and on rabbit plantaris muscle (Greaser *et al.* 1988). The discrepancy might be explained by the observation (Maxwell, Faulkner & Lieberman, 1973) that cross-sectional area depends strongly on the muscle of origin and on the age of the animal.

Isometric tension development was found to be lower in slow fibres than in fast fibres. This is in accordance with the results of Eddinger & Moss (1987), but not with those of Greaser *et al.* (1988). Regarding the differences among fast fibres, the few data available (Eddinger & Moss, 1987; Greaser *et al.* 1988) suggest that type 2B fibres are stronger than type 2A. Our data did not show any statistically significant difference among type 2 fibres.

Force–velocity measurements

The signals of the length change during isotonic shortening (shown in Fig. 1) exhibited a clear curvature, as has been shown in previous studies (Brenner, 1980, 1986; Ferenczi, Goldman & Simmons, 1984). Thus, velocity is a function of time at which measurements are made: i.e. the later they are made the slower the velocity obtained. The initial speed of shortening obtained by extrapolation to the beginning of the shortening phase should be the only value of velocity unaffected by curvature (Brenner, 1986). In this study shortening velocity was measured 30–40 ms after the beginning of the length change, when length and tension oscillations had disappeared. According to Ferenczi *et al.* (1984) little difference should be found between the initial speed of shortening (determined by extrapolation) and velocity measured early

during shortening (as in the present work). In this study velocity values were used only for comparison between different fibre types. No obvious difference in curvature of length traces in different fibre types was seen. On the other hand, the curvature of the shortening traces was consistently greater at low loads than at high loads. This might cause an underestimation of shortening velocity at low loads (see below).

The values of V_0 obtained in this study are comparable to others previously measured in single skinned fibres of rat diaphragm and leg muscles by Eddinger & Moss (1987), Eddinger, Cassens & Moss (1986) and Reiser, Kasper, Greaser & Moss (1988). Velocity measurements reported in these studies using the slack-test method at 15 °C ranged from 0·66 to 5·38 L/s. These values are comparable with those obtained in this study taking into account the difference in temperature and the discrepancy between the slack-test and load-clamp procedures for the determination of V_0 (Julian, Rome, Stephenson & Striz, 1986).

Shape of the force–velocity curve

In intact skeletal muscle fibres, the force–velocity relation curve deviates, at very high and very low loads, from the hyperbola fitted with Hill's equation (Edman *et al.* 1976; Julian *et al.* 1986; Edman, 1988). Velocity points fall below the hyperbola at high loads and above the hyperbola at low loads. In contrast, force–velocity curves obtained in skinned frog fibres did not show any departure from the hyperbola at high loads (Julian *et al.* 1986). The results obtained in this study showed that velocities of type 1, 2B and 2X fibres at loads above 0·8 P_0 were even above the hyperbola. Computed P_0^* values were in fact lower ($P_0^*/P_0 = 0{\cdot}879$) than isometric force (P_0). Unexpectedly force–velocity curves of type 2A fibres did not depart from the hyperbola at very high loads ($P_0^*/P_0 = 1{\cdot}027$). No simple explanation can be given at present for the difference between intact and skinned fibres and for the surprising difference between type 2A and the other fibre types.

In this study, at low loads, data points fell very close to the hyperbolae fitted to all the velocity points. The value of V_0 obtained by Hill's hyperbolic equation was consistently higher than the value of V_0 obtained by linear extrapolation of data points below 0·1 P_0. This is in contrast to the findings of Julian *et al.* (1986). Species differences or possible underestimation of shortening velocity due to the higher curvature of length records at low loads might explain the differences.

Since maximum shortening velocity values critically depend on the way force–velocity points are extrapolated, our conclusions concerning the relationship between MHC composition and shortening velocity might be affected by the method of calculating V_0. To check this, values of V_0 obtained by linear extrapolation of data points below 0·1 P_0 were plotted in a histogram like the one in Fig. 6. The relation between shortening velocity and fibre type was the same, although all V_0 values were reduced.

Shortening velocity and myosin heavy chain composition

The results reported in this paper show that there was a continuum in maximum shortening velocity among individual rat fibres from EDL, soleus and plantaris muscles, regardless of the fibre origin. Within this continuum four different fibre groups according to MHC compositions were identified. Only slow fibres containing

type 1 MHC could be unequivocally identified by their velocity of shortening which was in all cases below 0·95 L/s.

Ranges of shortening velocity of fast (type 2A, 2B and 2X) fibres mostly overlapped. Mean values of shortening velocity of fast fibres seem to suggest that type 2B MHC might be associated with higher velocities of shortening than type 2A and 2X MHC. However, the histogram in Fig. 6 clearly shows that only one group of type 2B fibres is definitely faster than the majority of fast fibres having shortening velocities between 0·90 and 2·10 L/s.

The variability of V_0 within each fibre type was very wide and beyond that which could be expected from possible experimental errors. A similar large variability (0·5–1·0 L/s) among fibres with a homogeneous type 1 MHC content can be noted in Fig. 2 of Reiser *et al.* (1985).

In the attempt to explain these results two different hypotheses can be forwarded. One hypothesis is that muscle fibres shorten at different velocities because they contain different MHC isoforms. Support for this hypothesis is given by a number of studies carried out on both cardiac and skeletal muscles (Mercandier *et al.* 1981; Reiser *et al.* 1985, 1988; Edman *et al.* 1988). V_0 was found to vary with the content of fast MHCs when occasionally co-expressed with the predominant slow MHCs in slow fibres from rabbit (Reiser *et al.* 1985). In avian slow fibres, V_0 was related to the ratio between two different isoforms of slow MHCs (Reiser *et al.* 1988). The clear difference in V_0 between slow and fast fibres presented in Table 3 and shown in Fig. 5 of this study confirms the previous observation that, at least under some conditions, V_0 is related to MHC composition. On the other hand, the large variability within the same fibre type and the overlapping shortening velocity among different fast fibre types reported in the present study cannot be readily explained along these lines. Co-existence of different MHCs in the same fibre might provide an explanation. Monoclonal antibodies very precisely identify the predominant MHC isoform expressed in a muscle fibre. The co-existence of MHCs in small amounts (Danieli-Betto *et al.* 1986; Staron & Pette, 1987*a*, *b*; Termin *et al.* 1989) can, however, remain undetected (see Methods). Fibres classified as type 1 and 2X should contain only one kind of MHC isoform. Fibres classified as type 2A and 2B might contain various amounts of 2X MHC. Co-existence of MHCs might therefore explain the large variability in shortening velocity within type 2A and 2B, but not within type 1 and 2X. The variability within the latter groups, and by extension also within the other groups, might be explained by the existence of more than four MHC isoforms in skeletal muscle fibres (Schmitt & Pette, 1990).

A second possibility is that contractile proteins other than MHCs can be at least partially responsible for the variability in shortening velocity. Alkali MLCs are interesting candidates. Evidence in favour of MLC's role has been given by studies in which either V_0 has been related to the MLC1f/MLC3f ratio (Sweeney *et al.* 1988; Greaser *et al.* 1988) or V_0 has been evaluated in fibres subjected to extraction of various amounts of MLC1f or MLC3f (Moss, Reiser, Greaser & Eddinger, 1990). Fast MLCs are expressed only in fast fibres, that is together with type 2A, B or X MHCs (Staron & Pette, 1987*b*), and slow MLCs are expressed only in slow fibres (with the exception of type 2A fibres in slow muscles that can contain various amounts of MLCs; Staron & Pette, 1987*a*). Differences in shortening velocity observed in this

study between slow and fast fibres and among fast fibres could be therefore due to differences in the kind (fast or slow) or in the proportion of MLCs (MLC1/MLC3 ratio). Very little is known about the impact of other contractile protein isoforms on the kinetics of contraction (Greaser *et al.* 1988).

In our opinion, the immunocytochemical method employed in this study identifies MHC composition of muscle fibres more precisely than in previous studies. None the less, a clear picture of the relation between shortening velocity and MHC isoforms does not emerge. The possible co-existence of MHC isoforms or the existence of still undetected MHC isoforms or a MLC contribution might explain the variation in V_0 within fibre types with apparently homogeneous MHC content.

Curvature of the force–velocity relation and maximum power output and myosin heavy chain composition

The curvature of the force–velocity relation quantified by a/P_0^* distinguished two groups of fibres: fibres containing type 1 MHC and 2A MHC which exhibited a high curvature (low a/P_0^*), and fibres containing type 2X MHC and 2B MHC which exhibited a low curvature (high a/P_0^*). The same two groups could also be identified according to maximum power output expressed relative both to P_0 and V_0 (P_{max}^{**}): type 1 and 2A (low power output), and type 2B and 2X (high power output). According to Woledge (1968) the higher the curvature and the lower the maximum power output the higher is the efficiency by which the muscle converts chemical into mechanical energy. The results reported in this paper suggest that thermodynamic efficiency is higher for type 1 and 2A fibres than for type 2B and 2X fibres.

Previous studies showed that V_0 and curvature were inversely related in whole muscles (Woledge, 1968; Close, 1969; Ranatunga, 1982), whereas no significant relation was found by Edman, Reggiani & te Kronnie (1985) in single frog fibres. Our results suggest that a/P_0^* values are not unequivocally related to shortening velocity.

Maximal power output expressed relative only to P_0 (P_{max}^*) provides information about the capacity of the contractile machine to perform mechanical work. Using this parameter, three groups of fibres were identified: a high power output group comprised of type 2B and 2X fibres, an intermediate power group comprised of type 2A fibres, and a low power group comprised of type 1 fibres. Thus, MHC composition seems important in determining the absolute capacity of the contractile material to produce mechanical work. However, fibres containing different MHCs (2B and 2X) showed similar P_{max}^* values. The difference between the isoforms 2B and 2X of MHC might have little influence on P_{max}^*. Alternatively other factors in addition to MHC composition may be involved in determining the muscle capacity to produce mechanical work as well as its shortening velocity.

We wish to thank Mr Luigi Guidotti and Mr Pierangelo Parona for invaluable technical assistance.

REFERENCES

BAR, A. & PETTE, D. (1988). Three fast myosin heavy chains in adult rat skeletal muscle. *Federation of European Biochemical Societies Letters* **235**, 153–155.

BRENNER, B. (1980). Effect of free calcium Ca^{2+} concentration on maximum unloaded shortening velocity: measurements on single glycerinated rabbit psoas muscle fibres. *Journal of Muscle Research and Cell Motility* **1**, 409–428.

BRENNER, B. (1983). Technique for stabilizing the striation pattern in maximally calcium-activated skinned rabbit psoas fibres. *Biophysical Journal* **41**, 99–102.

BRENNER, B. (1986). The necessity of using two parameters to describe isotonic shortening velocity of muscle tissues: the effect of various interventions upon initial shortening velocity (Vi) and curvature (b). *Basic Research in Cardiology* **81**, 54–69.

BROOKE, M. H. & KAISER, K. K. (1970). Three myosin adenosine triphosphatase systems: the nature of their pH lability and sulphydryl dependence. *Journal of Histochemistry and Cytochemistry* **18**, 670–672.

CLOSE, R. (1969). Dynamic properties of fast and slow skeletal muscles of the rat after nerve cross-union. *Journal of Physiology* **204**, 331–346.

DANIELI-BETTO, D., ZERBATO, E. & BETTO, R. (1986). Type I, IIa and IIb myosin heavy chain electrophoretic analysis of rat muscle fibres. *Biochemical and Biophysical Research Communications* **138**, 981–987.

EDDINGER, T. J., CASSENS, R. G. & MOSS, R. L. (1986). Mechanical and histochemical characterization of skeletal muscles from senescent rats. *American Journal of Physiology* **251**, C421–430.

EDDINGER, T. J. & MOSS, R. L. (1987). Mechanical properties of skinned single fibres of identified types from rat diaphragm. *American Journal of Physiology* **253**, C210–218.

EDMAN, K. A. P. (1988). Double-hyperbolic force–velocity relation in frog muscle fibres. *Journal of Physiology* **404**, 301–321.

EDMAN, K. A. P., MULIERI, L. A. & SCHUBON-MULIERI, B. (1976). Non-hyperbolic force–velocity relationship in single muscle fibres. *Acta Physiologica Scandinavica* **98**, 143–156.

EDMAN, K. A. P., REGGIANI, C., SCHIAFFINO, S. & TE KRONNIE, G. (1988). Maximum velocity of shortening related to myosin isoform composition in frog skeletal muscle fibres. *Journal of Physiology* **395**, 679–694.

EDMAN, K. A. P., REGGIANI, C. & TE KRONNIE, G. (1985). Differences in maximum velocity of shortening along single muscle fibres of the frog. *Journal of Physiology* **365**, 147–163.

FABIATO, A. (1988). Computer programs for calculating total from specific free or free from specified total ionic concentrations in aqueous solutions containing multiple metals and ligands. *Methods in Enzymology* **157**, 387–417.

FERENCZI, M. A., GOLDMAN, Y. E. & SIMMONS, R. M. (1984). The dependence of force and shortening velocity on substrate concentration in skinned muscle fibres from *Rana temporaria*. *Journal of Physiology* **350**, 519–543.

GODT, R. E. & MAUGHAN, D. W. (1977). Swelling of skinned muscle fibres of the frog. Experimental observations. *Biophysical Journal* **19**, 103–116.

GREASER, M. L., MOSS, R. L. & REISER, P. J. (1988). Variations in contractile properties of rabbit single muscle fibres in relation to troponin T isoforms and myosin light chains. *Journal of Physiology* **406**, 85–98.

IZUMO, S., NADAL GINARD, B. & MAHDAVI, V. (1986). All members of the MHC multigene family respond to thyroid hormone in a highly tissue-specific manner. *Science* **231**, 597–600.

JULIAN, F. J., ROME, L. C., STEPHENSON, D. G. & STRIZ, S. (1986). The maximum speed of shortening in living and skinned frog muscle fibres. *Journal of Physiology* **370**, 181–199.

MAXWELL, L. C., FAULKNER, J. A. & LIEBERMAN, D. A. (1973). Histochemical manifestations of age and endurance training in skeletal muscle fibres. *American Journal of Physiology* **224**, 356–361.

MERCANDIER, J. J., LOMPRE, A. M., WISNEWSKY, C., SAMUEL, J. L., BERCOVICI, J., SWYNGHEDAUW, B. & SCHWARTZ, K. (1981). Myosin isoenzymic changes in several models of rat cardiac hypertrophy. *Circulation Research* **49**, 525–532.

MOSS, R. L., REISER, P. J., GREASER, M. L. & EDDINGER, T. J. (1990). Varied expression of myosin alkali light chains is associated with altered speed of contraction in rabbit fast twitch skeletal muscles. In *The Dynamic State of Muscle Fibres*, ed. PETTE, D. pp. 355–368. Walter de Gruyter, Berlin, New York.

RANATUNGA, K. W. (1982). Temperature-dependence of shortening velocity and rate of isometric tension development in rat skeletal muscle. *Journal of Physiology* **329**, 465–483.

REISER, P. J., GREASER, M. L. & MOSS, R. L. (1988). Myosin heavy chain composition of single cells from avian slow skeletal muscle is strongly correlated with velocity of shortening during development. *Developmental Biology* **129**, 400–407.

REISER, P. J., KASPER, C. E., GREASER, M. & MOSS, R. L. (1988). Functional significance of myosin transitions in single fibres of developing soleus muscle. *American Journal of Physiology* **254**, C605–613.

REISER, P. J., MOSS, R. L., GIULIAN, G. G. & GREASER, M. L. (1985). Shortening velocity in single fibres from adult rabbit soleus muscles is correlated with myosin heavy chain composition. *Journal of Biological Chemistry* **260**, 9077–9080.

SCHIAFFINO, S., GORZA, L., SARTORE, S., SAGGIN, L., AUSONI, S., VIANELLO, M., GUNDERSEN, K. & LØMO, T. (1989). Three myosin heavy chain isoforms in type 2 skeletal muscle fibres. *Journal of Muscle Research and Cell Motility* **10**, 197–205.

SCHIAFFINO, S., SAGGIN, L., VIEL, A., AUSONI, S., SARTORE, S. & GORZA, L. (1986). Muscle fibre types identified by monoclonal antibodies to myosin heavy chains. In *Biochemical Aspects of Physical Exercise*, ed. BENZI, G., PACKER, L. & SILIPRANDI, N., pp. 27–34. Elsevier, Amsterdam.

SCHMITT, T. L. & PETTE, D. (1990). Correlation between troponin-T and myosin heavy chain isoforms in normal and transforming rabbit muscle fibres. In *The Dynamic State of Muscle Fibres*, ed. PETTE, D., pp. 293–302. Walter de Gruyter, Berlin, New York.

STARON, S. R. & PETTE, D. (1986). Correlation between myofibrillar ATP-ase activity and myosin heavy chain composition in rabbit muscle fibres. *Histochemistry* **86**, 19–23.

STARON, S. R. & PETTE, D. (1987*a*). The multiplicity of combinations of myosin light chains and heavy chains in histochemically typed single fibres. Rabbit soleus muscle. *Biochemical Journal* **243**, 687–693.

STARON, S. R. & PETTE, D. (1987*b*). The multiplicity of combinations of myosin light chains and heavy chains in histochemically typed single fibres. Rabbit tibialis anterior muscle. *Biochemical Journal* **243**, 695–699.

SWEENEY, H. L., KUSHMERICK, M. J., MABUCHI, K., SRÉTER, F. A. & GERGELY, J. (1988). Myosin alkali light chain and heavy chain variations correlate with altered shortening velocity of isolated skeletal muscle fibres. *Journal of Biological Chemistry* **263**, 9034–9039.

TERMIN, A., STARON, R. S. & PETTE, D. (1989). Changes in myosin heavy chain isoforms during chronic low-frequency stimulation of rat fast hindlimb muscles. *European Journal of Biochemistry* **186**, 749–754.

WOLEDGE, R. C. (1968). The energetics of tortoise muscle. *Journal of Physiology* **197**, 658–707.

WOLEDGE, R. C., CURTIN, N. A. & HOMSHER, E. (1985). Energetics aspects of muscle contraction. *Monographs of the Physiological Society*, No. 41. Academic Press, London.